Chemical Engineering Journal 161 (2010) 34–45

Contents lists available at ScienceDirect

Chemical Engineering Journal

journal homepage: www.elsevier.com/locate/cej

Adsorptive separation of *Ginsenoside* from aqueous solution by polymeric resins: Equilibrium, kinetic and thermodynamic studies

Pranab Barkakati [a,*], Ashma Begum [a], Makhan Lal Das [b], Paruchuri Gangadhar Rao [a]

[a] *Chemical Engineering Division, North East Institute of Science and Technology, Council of Scientific & Industrial Research, Jorhat 785 006, Assam, India*
[b] *Department of Chemical Engineering, Assam Engineering College, Jalukbari, Guwahati 781 013, Assam, India*

ARTICLE INFO

Article history:
Received 3 September 2009
Received in revised form 12 April 2010
Accepted 12 April 2010

Keywords:
Adsorption
Adsorbents
Kinetics
Shake-flask
Ginsenoside
Isotherm

ABSTRACT

The adsorption behaviour of Ginsenoside from aqueous solution onto polymeric resins such as XAD-4, XAD-7, XAD-16 and XAD-1180 was studied. Adsorption isotherms were interpreted from various isotherm models like Langmuir, Freundlich, Redlich–Peterson, Dubinin–Radushkevich and Temkin and their parameters were evaluated and compared. The adsorption kinetics was analyzed using series of rate equations like first-order rate equation, second-order rate equation, Bangham's model, Intra-particle diffusion model, Boyd's diffusivity model and Elovich kinetic equation. The adsorption performance was investigated thermodynamically under batch equilibrium conditions at 293, 298, 303 and 308 K. The optimum temperature of adsorption was observed to be 298 K. Studies of external mass transfer and pore diffusion effects revealed that both film and pore diffusion play significant role in different extent and stages of contact in the sorption process. The adsorption efficiency and uptake rates of Ginsenoside were compared and the highest adsorption efficiency was observed with XAD-7 (>90%). The removal effectiveness is in order of XAD-7 > XAD-16 > XAD-1180 > XAD-4. The rate of Ginsenoside removal better follows pseudo-second-order rate kinetic model, corroborating high correlation coefficients for calculated parameters with the experimental data.

1. Introduction

Ginseng is a well known oriental medicinal plant with wide biological activities. The triterpene derivatives called Ginsenosides, present in the Ginseng roots are the main pharmacoactive ingredients in Ginseng. They are known to exhibit immuno-modulatory and stimulatory effects facilitating both physical and mental activities on human health including antihypertensive, anticancer, anti-aging and hepato-protective effects [1–4]. However, extraction of the active Ginsenosides from the roots or cultured products [5] and their further purification encounters difficulties because of their presence in low amount and also complexity of the matrices [6]. Amberlite XAD polymeric adsorbents are highly porous spherical polymer beads based on cross-linked, macro-reticular polystyrene, aliphatic, or phenol-formaldehyde condensate polymers. Their high internal surface areas can adsorb and desorb a wide variety of different species depending on the environment in which they are used. Polymeric adsorbents are increasingly used for selective separation of biomolecules for their wide variations in functionality, surface area and porosity. The adsorption based separation techniques are one of the most promising methods for separation processes since they are non-denaturing, highly selective, energy efficient and relatively inexpensive and hence used for bulk separation and purification in food, pharmaceuticals and chemical industries. They are attractive due to their favourable elution and regeneration characteristics and have many advantages like low toxicity, effective separation from very dilute aqueous solutions and special selectivity. Extensive studies have been made on the adsorption of various bio-molecules on neutral polymeric resins [7–10]. There is, of course, no hint in the literature the application and effectiveness of Amberlite polymeric adsorbents in the separation of Ginsenosides from aqueous solutions of crude Ginseng extract.

Adsorption is a process of accumulation of molecules from a bulk solution onto the external and internal surfaces of the adsorbent. This process involves various interactions such as hydrophobic, electrostatic attraction and hydrogen bonding. The sorption capacity of the adsorbents strongly depends on the surface area, contact time, polarity, concentration and the degree of hydrophobicity in the adsorption system. The equilibrium adsorption isotherms depict the correlation between equilibrium concentration of the adsorbate in the solid and liquid phase at constant temperature and suggest the interactive forces operational in the process. The evaluation of the adsorption rate constants could assess the efficacy of the sorbents as well as determine the overall adsorption

* Corresponding author. Tel.: +91 376 2370121x2384; fax: +91 376 2370011.
E-mail addresses: barkakati@yahoo.com, barkakatip@rrljorhat.res.in (P. Barkakati).

1385-8947/$ – see front matter © 2010 Elsevier B.V. All rights reserved.
doi:10.1016/j.cej.2010.04.018

Table 1
Properties of Amberlite polymeric adsorbents.

Properties	XAD-4	XAD-7	XAD-16	XAD-1180
Chemical nature	Polystyrene divinyl benzene	acrylic ester	Polystyrene divinyl benzene	Polystyrene divinyl benzene
Polarity	Non-polar	Weakly polar	Non-polar	Non-polar
Porosity	0.51	0.55	0.55	0.60
Pore volume ($cm^3\ g^{-1}$)	0.97	1.14	1.40	1.68
Particle size (mm)	0.49–0.69	0.25–0.84	0.30–1.20	0.35–0.60
Mean pore dia (Å)	50	80	100	140
Density ($g\ ml^{-1}$)	1.04	1.07	1.02	1.04
Surface area ($m^2\ g^{-1}$)	750	450	825	600

performance for designing a sorption system. Another practice in the adsorption study is the fitting of the experimental data with different isotherm model equations for prediction of a suitable model for the adsorption process design.

In this paper, the feasibility of using micro-porous polymeric adsorbents as a simple and effective tool for separation and purification of Ginsenosides from aqueous solutions has been discussed. The work reports experimental data on the batch equilibrium adsorption of Ginsenoside from aqueous solutions at various concentrations and temperature on to Amberlite neutral resins of different properties. The isotherms were established and the experimental data points were compared to different isotherm models. The diffusivity and the adsorption capacities of the resins were estimated and the enthalpy and free energy of adsorption were also evaluated.

2. Materials and methods

2.1. Adsorbents and their properties

The polyaromatic adsorbents used in the study are Amberlite XAD-4, XAD-7, XAD-16 and XAD-1180. While XAD-4, 7 and 16 were procured from Fluka Chemika, France, XAD-1180 resin was supplied by Acros Organics, NJ, USA. The physical properties and characteristics of the resins as available from the manufacturer are reported in Table 1. Ginseng dry extract samples were acquired from Himedia Laboratories, Mumbai, India. Potassium dihydrogen orthophosphate and dipotassium hydrogen phosphate were obtained from Central Drug House, Mumbai, India.

2.2. Adsorbate (Ginsenoside) and its preparation

Standard solutions of Ginsenoside in the range of 0.085–0.425 $g\ L^{-1}$ concentrations were prepared using known weight of Giseng dry extract in specific volumes of de-ionized water (Millipore Milli-Q).

2.3. Analytical methods

The resins were washed with deionized water (Millipore Milli-Q) several times to remove any NaCl and Na_2CO_3 and dried at 323 K in a hot air circulating electrical oven for 6 h and kept in desiccator to reach ambient temperature until use. Ginsenoside was analyzed by UV visible spectrometry in the range 193–203 nm using Shimadzu UV-1601PC spectrophotometer and cross checked by chromatography in HPLC (Waters) on a reverse phase Luna C-18 (2) column with water:acetonitrile as eluent for detection at λ_{max} 203 nm and flow rate of 1 $ml\ min^{-1}$. A calibration graph was plotted for the spectrometric assay of Ginsenoside using an external standard. UV spectrophotometry is one of the various techniques for analysis and detection of Ginsenosides [11,12]. Because of the weak UV absorption of Ginsenosides, their detection is usually achieved at 193–203 nm. Phosphate buffers are used at pH 5.8 for the detection process and the concentration of the phosphate buffer is important in order to obtain the separation of Ginsenosides.

2.4. Adsorption equilibrium and kinetics

The time dependent adsorption studies were conducted by adding 0.1 g of each of the resins to 20 ml of 0.33 g/L of aqueous Ginsenoside solution. Adsorption was carried out in a temperature controlled orbital shaker (Kühner AG IRC-1-U) at 200 rpm and 298 K. Each experiment was continued for a definite period of adsorption from 1 to 24 h, and after each experiment the adsorbents were removed by paper filtration and the left over Ginsenoside in the solution was estimated analytically. The equilibrium adsorption capacity was calculated following the mass balance equation (1).

$$q_e = (C_0 - C_e)\frac{V}{m} \tag{1}$$

where q_e is the equilibrium solute phase concentration in solute mass/adsorbent mass; C_0 is the initial liquid phase concentration in solute mass/solution volume; C_e is the equilibrium solute phase concentration in aqueous phase in solute mass/solution volume; V is the volume of the solution and m is the mass of the adsorbent used.

For the establishment of the equilibrium adsorption isotherm, experimental data points were obtained by contacting known amount of each of the adsorbents (XAD-4, XAD-7, XAD-16 and XAD-1180) with solutions of varying Ginsenoside concentration for a fixed period of time to achieve the equilibrium. 0.2 g of the adsorbents were added to 20 ml of aqueous solution of 0.085–0.40 g/L concentration of Ginsenoside and adsorption reactions were carried out at 298 K for 18–24 h in a temperature-controlled orbital shaker (Kühner AG IRC-1-U) at 200 rpm when equilibrium conditions were reached. At the end of the reaction, the sorbents were removed from the solution by paper filtration and the residual Ginsenoside concentration in the solution was estimated analytically.

2.5. Adsorption isotherm modeling

The equilibrium data obtained at a temperature of 298 K for adsorption of Ginsenoside onto the polymeric adsorbents were analyzed using the following isotherm model equations.

2.6. Langmuir isotherm

The Langmuir isotherm model [13] is based on monolayer coverage of adsorbent surfaces by the adsorbate at specific homogeneous sites within the adsorbent and is represented as

$$q_e = \frac{q_m K_L C_e}{1 + K_L C_e} \tag{2}$$

where q_e is the equilibrium concentration of the adsorbate on the adsorbent in mg/g; C_e is the equilibrium concentration of the solute in liquid phase expressed as $mg\ L^{-1}$; q_m ($mg\ g^{-1}$) and K_L ($L\ mg^{-1}$)

are the Langmuir equation constants, representing the maximum adsorption capacity and adsorption energy parameter respectively. The equation can be linearized as given in (3) and plotting C_e/q_e versus C_e will give a straight line with $1/q_m$ as slope and $1/q_mK_L$ as intercept.

$$\frac{C_e}{q_e} = \frac{1}{q_m K_L} + \frac{C_e}{q_m} \tag{3}$$

The model (3) was tested with the equilibrium adsorption data of Ginsenoside adsorption on different adsorbents by the plot of C_e/q_e versus C_e.

2.7. Freundlich isotherm

The basic isotherm model developed by Freundlich [14] is based on multilayer adsorption of adsorbate onto the heterogeneous surfaces with a non-uniform distribution of heat of adsorption over the adsorbent surfaces and is represented by the equation

$$q_e = K_F {C_e}^{1/n} \tag{4}$$

where q_e and C_e are the solute phase concentrations in solid and liquid phases respectively as defined earlier and K_F and n are the Freundlich equation parameters. The linearized form of the Freundlich equation is given by

$$\log\ q_e = \log K_F + \frac{1}{n} \log C_e \tag{5}$$

A plot of $\log q_e$ versus $\log C_e$ of the linearized equation (5) should result in a straight line whose slope and intercept would determine the values of n and K_F. The Freundlich isotherm is derived by assuming a heterogeneous surface. The Freundlich model equation (5) was tested by the plot of $\ln q_e$ against $\ln C_e$ for all the four adsorbents under study.

2.8. Redlich–Peterson isotherm

The Redlich–Peterson isotherm [15] has a linear dependence on concentration and an exponential function in the denominator. It approaches the Freundlich model at high concentration and is in concurrence with the low concentration limit of the Langmuir equation. The Redlich–Peterson equation is represented as

$$q_e = \frac{K_R C_e}{1 + a_R C_e^{\beta}} \tag{6}$$

where a_R $(L\,mg^{-1})^{-1/\beta}$ and K_R $(L\,g^{-1})$ are isotherm constants and exponent β lies between 0 and 1. For $\beta = 1$ the equation reduces to Langmuir equation and for $\beta = 0$ it is reduced to Henry's equation. The linear form of the Redlich–Peterson equation is obtained by taking logarithm and is

$$\ln\left(K_R \frac{C_e}{q_e} - 1\right) = \ln\ a_R + \beta \ln C_e \tag{7}$$

The three parameters of equation (7) viz. a_R, β and K_R are used to analyze the experimental data via linear regression with trial and error optimization of β to yield the maximum regression coefficient value R^2.

2.9. Dubinin–Radushkevich isotherm

The Dubinin–Radushkevich isotherm [16] assumes that the characteristics of the sorption curves are related to porosity of the adsorbents and is represented by the following equation

$$q_e = Q_D\ \exp(-B_D\varepsilon^2) \tag{8}$$

where Q_D $(mg\,g^{-1})$ is the Dubinin–Radushkevich isotherm constant and ε $(kJ\,mol^{-1})$ is the Polanyi Potentiali. The Polanyi Potentiali, ε is correlated as

$$\varepsilon = RT\ \ln\left(1 + \frac{1}{C_e}\right) \tag{9}$$

where R is the gas constant $(8.314 \times 10^{-3}\,kJ\,mol^{-1}\,K^{-1})$ and T is temperature (K). B_D $(mol^2\,kJ^{-2})$ is related to mean free energy of sorption E $(kJ\,mol^{-1})$ and is correlated by the following equation

$$E = \frac{1}{\sqrt{2B_D}} \tag{10}$$

The Dubinin–Radushkevich isotherm constant can be estimated from the plot of the linear form of equation (8) as

$$\ln\ q_e = \ln\ Q_D - B_D\varepsilon^2 \tag{11}$$

2.9.1. Temkin isotherm

The Temkin isotherm model [17] has been developed in consideration with the chemisorption of the adsorbate onto the adsorbent. The model assumes that the heat of adsorption of all the molecules in the layer decreases linearly with the coverage due to adsorbate-adsorbent interactions. The equation and its linearized form are represented as follows:

$$q_e = \frac{RT}{b}\ \ln(K_T C_e) \tag{12}$$

$$q_e = B_1 \ln K_T + B_1 \ln C_e \tag{13}$$

where $B_1 = RT/b$, b $(mol\,kJ^{-1})$ is the Temkin isotherm constant, K_T $(L\,mg^{-1})$ is equilibrium binding constant, q_e $(mg\,g^{-1})$ and C_e $(mg\,L^{-1})$ are the solute concentrations in solid and liquid phases respectively, T (K) is temperature and R $(8.314 \times 10^{-3}\,kJ\,mol^{-1}\,K^{-1})$ gas constant. The isotherm parameters, b and K_T can be calculated from the slope and intercept of the linear plot of q_e versus $\ln C_e$ in Eq. (13).

2.10. Adsorption kinetics model equations

In an attempt to express the mechanism of Ginsenoside adsorption onto the surface and pores of the polymeric resins, the following kinetic model equations are used to analyze the adsorption experimental data for determination of the related kinetic parameters.

2.11. Pseudo-first-order model

The pseudo-first-order rate expression based on solid capacity is the most widely used rate equation for assigning the adsorption rate of an adsorbate from a liquid phase and is known as the Lagergren rate equation [18]. It is represented as

$$\frac{dq}{dt} = k_f(q_e - q) \tag{14}$$

where q_e $(mq\,g^{-1})$ and q $(mg\,g^{-1})$ are the adsorption capacity at equilibrium and time t respectively and k_f (min^{-1}) is the rate constant of the pseudo-first-order adsorption reaction. On integration and applying boundary conditions as $q = 0$ at $t = 0$ and $q = q_e$ at $t = t$, Eq. (14) becomes

$$\log(q_e - q) = \log\ q_e - \frac{k_f t}{2.303} \tag{15}$$

The value of the adsorption rate constant k_f is determined from the linear plot of $\log(q_e - q)$ against t.

2.12. Pseudo-second-order model

The pseudo-second order kinetic expression was developed by Ho and McKay [19] to describe the adsorption of metal ions onto adsorbents. The rate expression is represented as

$$\left(\frac{dq}{dt}\right) = k_s(q_e - q)^2 \tag{16}$$

where q_e and q (mg g^{-1}) are the adsorption capacities at equilibrium and time t respectively and k_s (g mg^{-1} min^{-1}) is the rate constant for the pseudo-second-order adsorption reaction. The integrated second order rate equation, at boundary conditions $q = 0$ at $t = 0$ and $q = q_e$ at $t = t$, becomes

$$\frac{t}{q} = \frac{1}{k_s q_e^2} + \frac{t}{q_e} \tag{17}$$

The value of q_e and k_s can be calculated from the linear plot of Eq. (17). The initial adsorption rate can be obtained as q/t, when t approaches zero. This is expressed as

$$h = k_s q_e^2 \tag{18}$$

where h is the initial adsorption rate and is expressed in mg g^{-1} min^{-1}.

2.13. Bangham's equation

The Bangham model [20] of adsorption kinetic studies tests out if the pore diffusion is the only rate controlling step. The model can be represented by the following equation

$$\log\left\{\log\left(\frac{C_b}{C_b - q_t m}\right)\right\} = \log\left(\frac{k_0 m}{2.303V}\right) + \sigma \ \log(t) \tag{19}$$

where C_b (mg) is the amount of initial adsorbate in the liquid phase, q_t (mg g^{-1}) is the concentration of solute in solid phase at any time t (min), m (g) is the amount of adsorbent, V (L) is the volume of solution used and k_0 (L g^{-1}) and σ (<1) are the Bangham's equation parameters.

2.14. Intra-particle diffusion model

The Weber's diffusion model [21] is the most commonly used technique for identifying the mechanism involved in the adsorption process. During the process of adsorption, the transportation of the adsorbate particles to the surface of the adsorbent surface takes place in several steps. The adsorption process may be controlled by film or external surface diffusion, pore diffusion, surface diffusion and adsorption on the pore surface or a combination of one or more steps. In a rapidly stirred batch process, the diffusive mass transfer can be related by an apparent diffusion coefficient which will fit experimental adsorption rate data. Usually a process is diffusion-controlled if its rate is dependent on the rate at which the components diffuse towards each other. The Weber's diffusion model is expressed as

$$q_t = k_d t^{1/2} + I \tag{20}$$

where q_t (mg g^{-1}) is concentration of adsorbate in solid phase at time t (min) and k_d (mg g^{-1} min$^{-½}$) is the intra-particle diffusion rate constant. A linear plot of q_t versus $t^{½}$ will give I as the intercept which gives an idea about the thickness of the boundary layer on the adsorbent surface. The larger the value of I, the greater is the boundary layer effect.

2.15. Boyd's diffusivity model

Boyd's kinetic model [22] for adsorption reaction is based on diffusion through the boundary liquid film, considering adsorption kinetics as a chemical phenomenon. The simplified form of the rate equation can be expressed as

$$\ln\left[\frac{1}{1 - F^2(t)}\right] = \frac{\pi^2 D_e t}{R_a^2} \tag{21}$$

where $F(t) = q_t/q_e$ is the fractional attainment of equilibrium at time t, D_e (m^2 s^{-1}) is the rate constant and R_a (m) is the radius of the spherical adsorbent particle. A linear plot of $\ln[1/\{1 - F^2(t)\}]$ versus t will give the value of D_e.

2.16. Elovich kinetic model

The Elovich kinetic model [23] is based on chemisorption phenomena. It is expressed as

$$\frac{dq}{dt} = \alpha \ \exp(-\omega q) \tag{22}$$

In order to simplify the Elovich equation (20), Chine and Clayton [24] assumed that $\alpha\omega t \gg 1$, and when the boundary conditions $q = 0$ at $t = 0$ and $q = q$ at $t = t$, are applied the equation becomes

$$q = \frac{1}{\varpi}\ln(\alpha\varpi) + \frac{1}{\varpi}\ln t \tag{23}$$

where q (mg g^{-1}) is the adsorbate in solid phase at time t (min), α is the initial adsorption rate and ω is the adsorption rate. Eq. (23) can be rearranged as

$$q = A_1 + B_1 \ \ln t \tag{24}$$

where $A_1 = \ln(\alpha\omega).1/\omega$ and $B_1 = 1/\omega$. From the linear plot of Eq. (24) the values of A_1 and B_1 can be evaluated as intercept and slope of the straight line.

2.17. Effect of adsorbent concentration on adsorption efficiency

Different amounts of the resins XAD-4, XAD-7, XAD-16 and XAD-1180 in concentrations of 5–25 g L^{-1} were added to 20 ml of 0.33 g L^{-1} aqueous solution of Ginsenoside in 250 ml Erlenmeyer flasks and adsorption was carried out at 200 rpm in the orbital shaker at 298 K for 18–24 hrs till the equilibrium is reached. The efficiency of the adsorption process was estimated as the ratio of the mass of Ginsenoside adsorbed to the mass of the adsorbent.

2.18. Effect of temperature on adsorption

The effect of temperature on adsorption of Ginsenoside on polymeric adsorbents was studied on two of the adsorbents, XAD-7 and XAD-16. 0.2 g of each of the adsorbents was contacted to 20 ml of four different concentrations of aqueous Ginsenoside solution in the range of 0.10–0.33 g L^{-1}. The experiments were carried out four different temperatures of 293, 298, 303 and 308 K in a temperature controlled orbital shaker at 200 rpm for 24 h. At the end of each experiment the adsorbents were separated by paper filtration and Ginsenoside in solution was analytically assayed.

2.19. Thermodynamic study

Considering the activity coefficient to be unity at low solute concentration as per Henry's law, the thermodynamic parameters for the adsorption process was calculated using the following thermodynamic relations

$$\Delta H^\circ = T\Delta S^\circ + \Delta G^\circ \tag{25}$$

and

$$\Delta G^\circ = -RT \ \ln K_0 \tag{26}$$

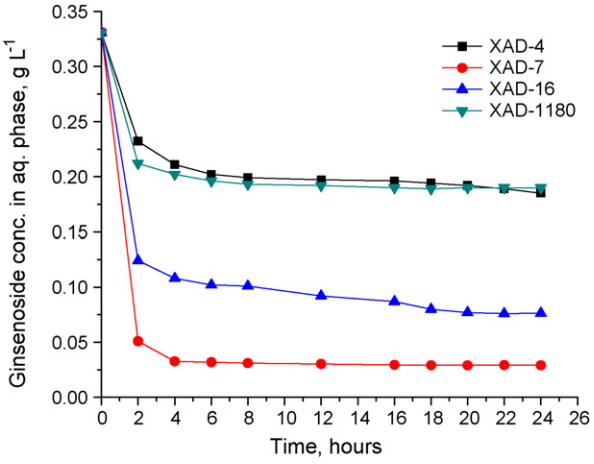

Fig. 1. Effect of contact time for adsorption of Ginsenoside on resins.

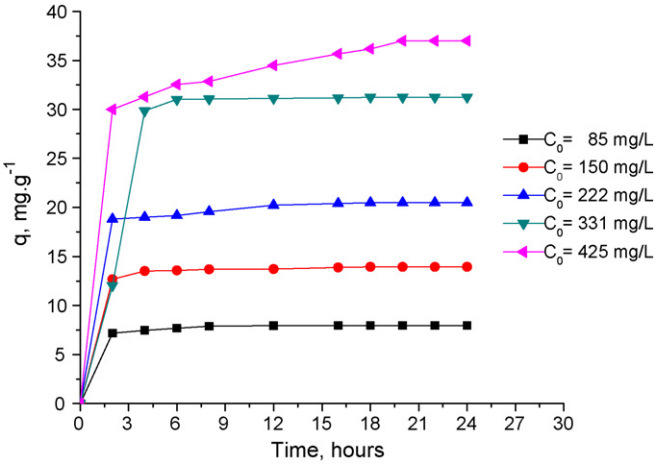

Fig. 2. Effect of initial concentration on the adsorption of Ginsenoside onto XAD-7.

Eqs. (25) and (26) can be combined as follows

$$\ln K_0 = \frac{\Delta S^\circ}{R} - \frac{\Delta H^\circ}{RT} \quad (27)$$

or

$$\ln \frac{C_{ad}}{C_e} = \frac{\Delta S^\circ}{R} - \frac{\Delta H^\circ}{RT} \quad (28)$$

where K_0 is the equilibrium constant at temperature T (K) and is equal to the adsorption affinity C_{ad}/C_e. C_{ad} (mg L^{-1}) is the reduction of adsorbate concentration of solution at equilibrium and C_e (mg L^{-1}) is the equilibrium concentration of the adsorbate in liquid phase. ΔH° (kJ mol^{-1}), ΔG° (kJ mol^{-1}) and ΔS° (kJ mol^{-1} K^{-1}) are the change in enthalpy, free energy and entropy at standard states respectively. R (8.314×10^{-3} kJ mol^{-1} K^{-1}) is gas constant. Assuming ΔH° and ΔS° to be constants within the studied temperature range, their values can be calculated from the slope and intercept of the straight line in the linear plot of ln C_{ad}/C_e versus $1/T$ and the change in free energy ΔG° at various temperatures are calculated from Eq. (25).

3. Results and discussions

3.1. Adsorption examination

The effect of contact period for the adsorption of Ginsenoside onto the resins is plotted as residual concentration of solute in liquid phase at C_0 of 0.33 g L^{-1} against time in Fig. 1. The result indicates that the uptake of Ginsenoside is rapid during the initial phase of 2 h of the contact time, and thereafter, becomes slower near the equilibrium. In between these final and initial stages of adsorption the rate is found to be virtually consistent. This is apparent from the fact that a large number of vacant surface sites are available for adsorption during the initial stage, and after a fall of time, the residual vacant sites are difficult to be occupied due to repulsive forces between the solute molecules on the solid and bulk phases. No significant change in Ginsenoside removal is observed after about 6 h except in case of XAD-16, where the rate of removal continued steadily till around 18 h of contact. This may be because of the highest surface area of XAD-16 amongst the range of Amberlite resins used in the study. It has also been observed that the adsorption efficiency of Ginsenoside by the resins is high and significant in case of XAD-7 and XAD-16 where the percentage removal is recorded as 91.2% and 76.9% respectively. The removal effectiveness is in the order of XAD-7 > XAD-16 > XAD-1180 > XAD-4.

The results on the rate of Ginsenoside adsorption onto the polymeric adsorbents XAD-7 and 16 as a function of the initial Ginsenoside concentration are shown in Figs. 2 and 3. The Ginsenoside adsorption was fast up to 2 h in case of XAD-7 and 4 h in case of XAD-16. Thereafter the adsorption was found to be slow. The time required to reach equilibrium was also observed to be more at higher initial concentrations. The adsorption onto both the resins, XAD-7 and XAD-16 was better and considerably uniform at 0.33 g L^{-1} concentration.

The effect of varying doses of the adsorbents XAD-4, XAD-7, XAD-16 and XAD-1180 was investigated using 0.33 g L^{-1} of Ginsenoside concentration at 298 K temperature. Fig. 4 shows an increase in the percentage of removal of Ginsenoside with the increase in dose of the adsorbents up to certain limit and then the rate of change in increase becomes negligible. The increase in the adsorption with increasing doses of adsorbents is likely due to increase in adsorbent surface area and availability of more adsorption sites. The optimum adsorbent doses for all the adsorbents were found to be 10–15 g L^{-1} of Ginsenoside solution.

3.2. Adsorption equilibrium studies

To optimize the design of the adsorption system for the adsorption of Ginsenoside onto various adsorbents the establishment of the most appropriate relationship for the equilibrium curves is very much essential. Various isotherm model equations have been used to describe the equilibrium characteristics of the Ginsenoside adsorption onto the studied polymeric adsorbents. The values of the estimated Langmuir isotherm parameters are given in Table 2

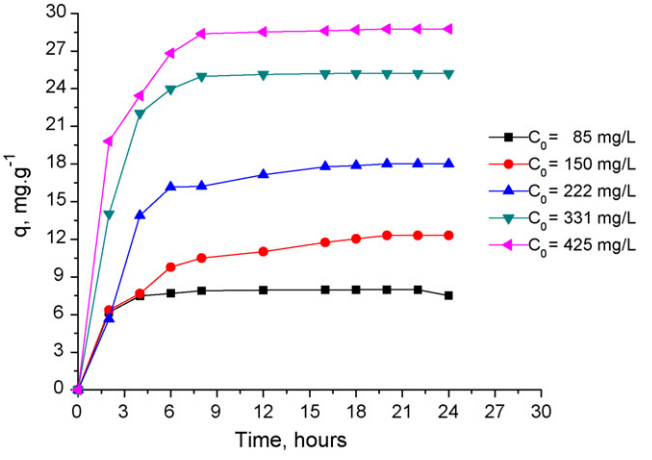

Fig. 3. Effect of initial concentration on the adsorption of Ginsenoside onto XAD-16.

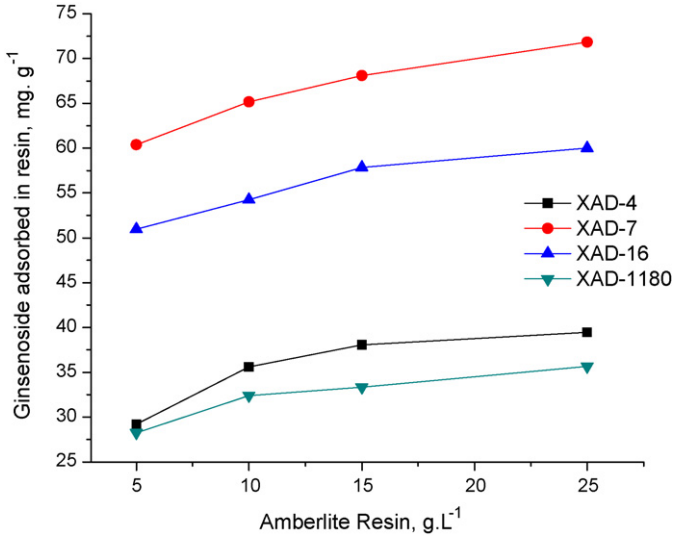

Fig. 4. Effect of adsorbent concentration for Ginsenoside adsorption on resins.

and the R^2 values are based on actual deviation between the experimental points and the theoretically predicted data points. It has been observed that the Langmuir isotherm equation more or less fits the experimental data points for all the adsorbents. The parameters indicate better adsorption capacity of XAD-7 for Ginsenoside adsorption.

The essential characteristics of the Langmuir isotherm can be expressed in terms of a dimensionless factor, R_L [25] which describes the type of isotherm and is defined as follows

$$R_L = \frac{1}{(1 + K_L C_0)} \quad (29)$$

If, $R_L > 1$, the adsorption is unfavourable; $R_L = 1$; the adsorption is linear; $0 < R_L < 1$, the adsorption is favourable and if $R_L = 0$, the system is irreversible. The values of R_L at $C_0 = 150\ \text{mg L}^{-1}$ are tabulated in Table 2 and they are found to be less than 1 for Ginsenoside adsorption on all the adsorbents verifying that the adsorption processes are favourable.

The Freundlich isotherm model equation (4) was examined by the plot of $\ln q_e$ versus $\ln C_e$ for the four adsorbents under test and the values of R^2 as shown in Table 2 are based on actual deviation of the experimental and theoretically predicted data points. Table 2 also shows the estimated Freundlich parameters for Ginsenoside adsorption on the adsorbents. The values of $1/n$ were observed to be less than unity for all the adsorbents indicating favourable adsorption [26].

There are two limiting factors in the Redlich–Peterson adsorption model for the variation of $\beta = 0$ (Langmuir form) and $\beta = 1$ (Henry's law). The Redlich–Peterson isotherm plots (not shown) for Ginsenoside adsorption onto the adsorbents indicate a better fitting of the equilibrium data for XAD-4 and XAD-1180. The values of the Redlich–Peterson isotherm parameters a_R, K_R, β and the correlation coefficient R^2 for adsorption of Ginsenoside onto the adsorbents are presented in Table 2. The values of β for all the adsorbents lie between 0 and 1, indicating favourable adsorption. The higher correlation coefficient values also signify well prediction of the experimental data by the R–P model.

The estimated values of the Dubinin–Radushkevich isotherm parameters for the adsorption of Ginsenoside are shown in Table 2. It is observed that the theoretical maximum adsorption capacity as evaluated using D–R equation is highest for the adsorbents XAD-7 and XAD-16. The mean free energy of adsorption, E estimated using the Polanyi Potentiali and the D–R isotherm constants were in the range of 0.04–0.26 kJ mol^{-1} which signifies of physical adsorption reaction due to weak Vander Waals forces. It is known that if the magnitude of the mean free energy lies between 8 and 16 kJ mol^{-1}, the mechanism of adsorption process can be explained by chemisorption or ion exchange [27]. It has also been observed that the values of the correlation coefficients for the D–R isotherm plots (not shown) are the lowest in comparison to the other four different isotherms model used for this study. It can therefore be determined that the D–R equation does not represent the experimental data satisfactorily.

The Temkin isotherm constants computed from the plots for Ginsenoside adsorption onto the resins are listed in Table 2. It is observed that the values of the correlation coefficients (R^2) are in the range of 0.97–0.98, signifying satisfactory representation of the equilibrium experimental data with the Temkin equation (12) for sorption model. It can therefore be presumed that the Ginsenoside adsorption is characterized by uniform distribution of binding energy and the heat of adsorption of the molecules in the layer decreases linearly with coverage of the adsorbate on the surface of the adsorbent particles [28].

In our present study we tried to use five different isotherm models provided by Langmuir, Freundlich, Redlich Peterson, Dubinin Radushkevich and Temkin to fit the experimental equilibrium data for aqueous Ginsenoside onto four different polymeric adsorbents, XAD-4,7,16 and 1180. The observed profiles of solid phase concentration of Ginsenoside at equilibrium, onto the resins against the liquid phase concentration C_e, indicate a good fit for the Langmuir, Freundlich, Redlich Peterson and the Temkin models to the experimental data as shown in Fig. 5. However, the profiles do not fit to the Dubinin Radushkevich model for adsorption onto all the resins in the higher range of equilibrium with the experimental data points.

Table 2
Isotherm parameters for Ginsenoside adsorption on various adsorbents.

Langmuir constants	q_m (mg g^{-1})	K_L (L mg^{-1})	R^2	R_L
Adsorbents				
XAD-4	17.3	0.024	0.99	0.217
XAD-7	63.9	0.027	0.97	0.197
XAD-16	39.4	0.021	0.99	0.244
XAD-1180	30.2	0.004	0.98	0.617

Freundlich constants	$1/n$	K_F (L mg^{-1})	R^2
Adsorbents			
XAD-4	0.327	2.56	0.98
XAD-7	0.670	2.87	0.98
XAD-16	0.531	2.32	0.97
XAD-1180	0.666	0.40	0.99

Redlich-Peterson constants	K_R (L g^{-1})	a_R (L mg^{-1})$^{-1/\beta}$	β	R^2
Adsorbents				
XAD-4	1.4	0.32	0.762	0.99
XAD-7	10.4	2.96	0.361	0.92
XAD-16	3.9	1.19	0.529	0.97
XAD-1180	2.1	4.80	0.347	0.99

Dubinin-Radushkevich constants	Q_D (mg g^{-1})	B_D (mol^2 kJ^{-1})	E (kJ mol^{-1})	R^2
Adsorbents				
XAD-4	12.8	42.9	0.108	0.76
XAD-7	28.5	7.4	0.259	0.79
XAD-16	22.4	21.3	0.153	0.73
XAD-1180	13.1	311	0.040	0.80

Temkin constants	B_1 (kJ^2 mol^{-2})	b (mol kJ^{-1})	K_T (L mg^{-1})	R^2
Adsorbents				
XAD-4	3.4	0.729	0.332	0.98
XAD-7	13.4	0.185	0.294	0.98
XAD-16	8.8	0.282	0.197	0.97
XAD-1180	6.2	0.397	0.044	0.98

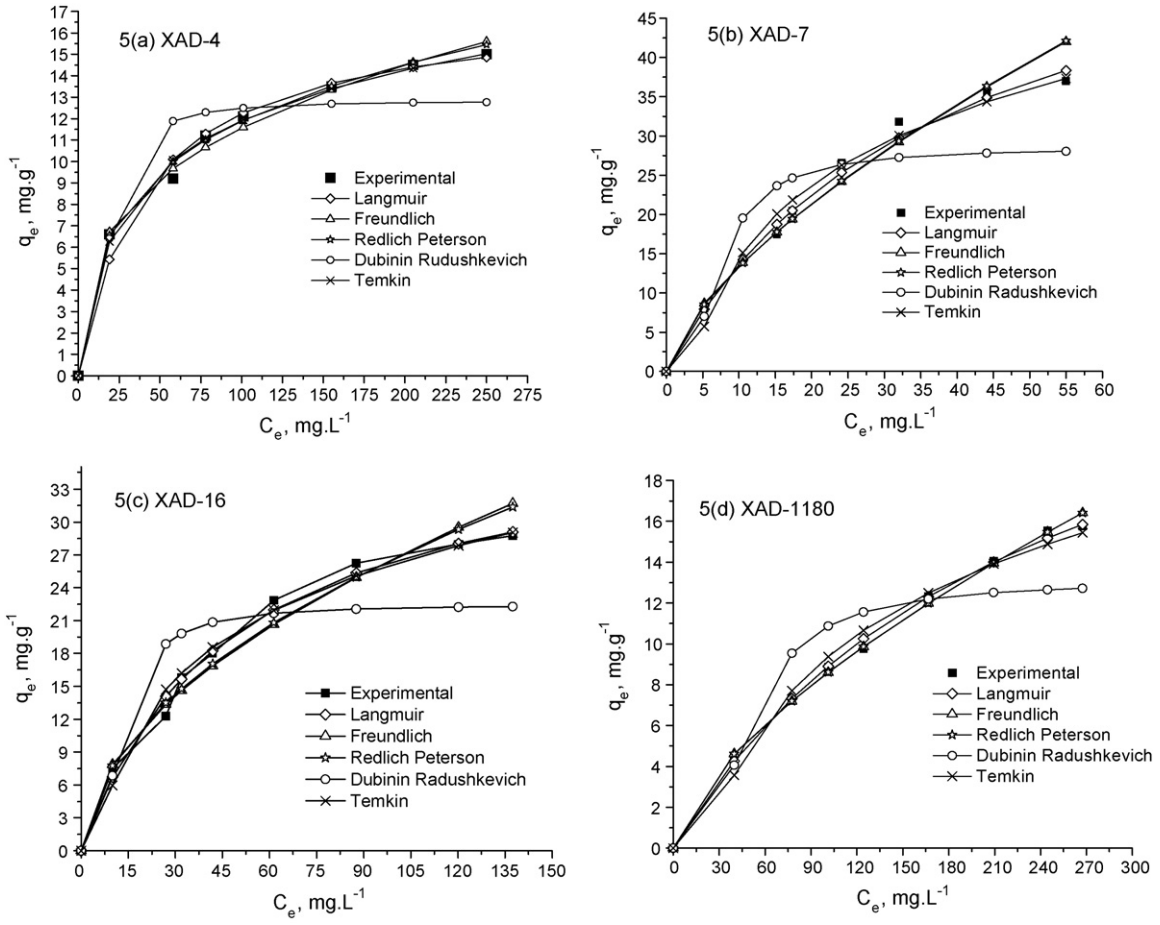

Fig. 5. Isotherms of Ginsenoside adsorption onto the resins.

From the comparison of the values for the correlation coefficients as determined by the standard statistical least square data reduction method for minimizing the deviations between the experimental and calculated values, the best fitting of the equilibrium data has been observed in the Freundlich, Langmuir and Temkin isotherms.

3.3. Adsorption kinetic study

The Ginsenoside adsorption data onto different resins were analyzed using various kinetic model equations like pseudo-first-order, pseudo-second-order, intra-particle diffusion, Boyd's diffusion model, Bangham kinetic model and Elovich model.

The values of the first-order rate constant k_f, for adsorption of Ginsenoside onto the adsorbents were calculated from the slope of the linear plots of log $(q_e - q)$ versus time also known as the Lagergren plot (Fig. 6). The adsorption capacity and the values of k_f are tabulated in Table 3. The plot and the calculated correlation coefficients (R^2) indicate that the rate of removal of Ginsenoside from the solution onto the adsorbents does not follow the pseudo-first-order equation.

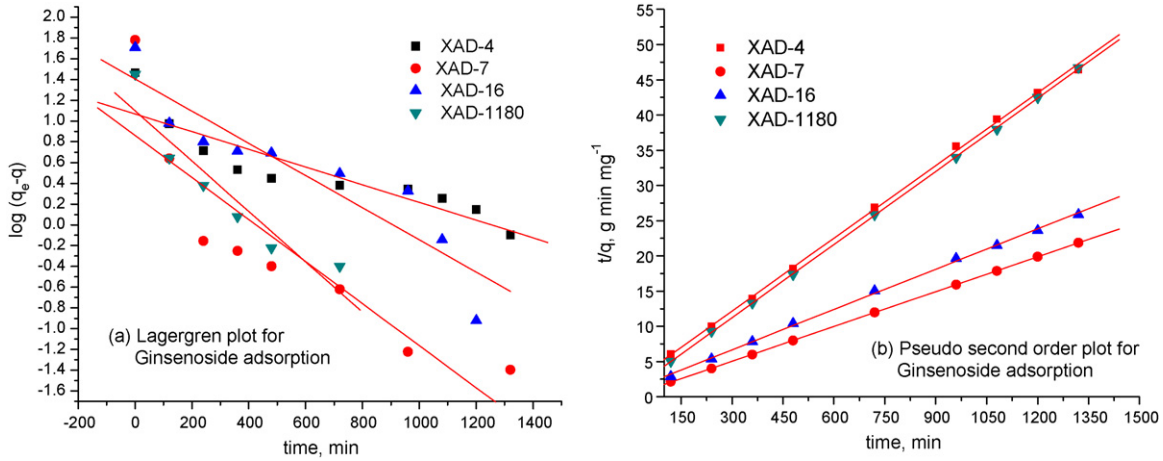

Fig. 6. Pseudo-first and -second-order plot for Ginsenoside adsorption onto the resins.

Table 3
Kinetic parameters for adsorption of Ginsenoside by various resins.

Pseudo-first order	k_f (min^{-1})	q_e (mg g^{-1}) calculated	q_e (mg g^{-1}) experimental	R^2
Adsorbents				
XAD 4	1.96×10^{-3}	2.91	29.2	0.82
XAD 7	4.68×10^{-3}	2.36	60.4	0.79
XAD16	3.57×10^{-3}	4.07	51.0	0.85
XAD1180	5.60×10^{-3}	3.00	28.3	0.88

Pseudo-second order	k_s (g mg^{-1} min^{-1})	h (mg g^{-1} min^{-1})	q_e (mg g^{-1}) (calculated)	q_e (mg g^{-1}) (experimental)	R^2
Adsorbents					
XAD 4	6.38×10^{-4}	0.54	29.1	29.2	0.99
XAD 7	2.56×10^{-3}	9.45	60.7	60.4	0.99
XAD16	3.78×10^{-4}	1.04	52.4	51.0	0.99
XAD1180	1.39×10^{-3}	1.16	28.9	28.3	0.99

Bangham's model	σ	k_0 (L g^{-1})	R^2
Adsorbents			
XAD 4	0.159	0.036	0.88
XAD 7	0.085	0.272	0.70
XAD16	0.163	0.090	0.97
XAD1180	0.087	0.061	0.90

Elovich model	ω	α	A_1	B_1	R^2
Adsorbents					
XAD 4	0.32	1.43×10^{2}	11.8	3.09	0.91
XAD 7	2.38	6.61×10^{58}	57.4	0.42	0.97
XAD16	0.26	1.49×10^{3}	23.0	3.86	0.96
XAD1180	0.81	9.93×10^{6}	19.6	1.23	0.87

Linear plots of t/q against time t as shown in Fig. 6 are used to estimate the values of k_s from the intercept of linear fit of the experimental points. The plots were observed to be linear and the calculated k_s values for XAD-4, XAD-7, XAD-16 and XAD-1180 at 298 K with their coefficients of deduction in linear regression analysis (R^2) are presented in Table 3. The correlation coefficients of all the data are found to be very encouraging in the range of R^2 >= 0.99, which corroborates that the adsorption of Ginsenoside onto the studied adsorbents follow the pseudo second order kinetic model. The calculated values of the solid phase solute concentration along with those of the experimental data are also presented in Table 3. The values are very close to each other signifying better approximation of the sorption data by the pseudo-second-order kinetic model than the first-order kinetic model for the sorption process by all the four adsorbents. It has also been observed that the values of h for the adsorption of Ginsenoside is highest in case of XAD-7 and is followed by XAD-1180 and XAD-16. It was observed that the adsorption rate for Ginsenoside on the resins were in the order of $k_{s(XAD\text{-}7)} > k_{s(XAD\text{-}1180)} > k_{s(XAD\text{-}16)} > k_{s(XAD\text{-}4)}$. Thus, the adsorption rate for XAD-7 is highest in comparison to those with XAD-1180, XAD-16 and XAD-4. The reason may be attributed to weak polarity for enhancing sorption rate in XAD-7 and slower rate of diffusion due to lower pore dia in XAD-4.

The kinetic data for Ginsenoside adsorption onto the Amberlite resins were analyzed by using the Bangham's equation to check if pore diffusion is the only controlling step in the adsorption process or not. The experimental data put to representation by equation (19) did not yield a desired linear fit in the double logarithmic plot as shown in Fig. 7. This indicates that the adsorption kinetics is not limited to only pore-diffusion or in other words the diffusion of the adsorbate into the pores of the adsorbents is not the only rate controlling step [29]. The values of the Bangham equation parameters σ and k_0 along with the correlation coefficients are given in Table 3. Results show highest value of k_0 for XAD-7 and the values of σ, less than unity for all the adsorbents. The values of the correlation coefficients also indicate poorer representation of the experimental data with the Bangham model. It may be possible that both film and pore-diffusion play significant role to different extent and stages of contact in the sorption process.

The kinetic data are also analyzed using the Elovich equation (22). The plot of solid phase adsorbate concentration versus ln t in rearranged Elovich equation (24) for the adsorption process at 298 K is shown in Fig. 8 and the model parameters determined along with their correlation coefficients are given in Table 3. The parameter values for XAD-7 are observed to be highest in the series.

3.4. Diffusivity study

The kinetic data were analyzed by the Weber's kinetic diffusion model represented by the intra-particle diffusion kinetic equation (20). Fig. 9 shows a plot of the mass of Ginsenoside adsorbed per unit mass of the adsorbents versus the square root of the contact

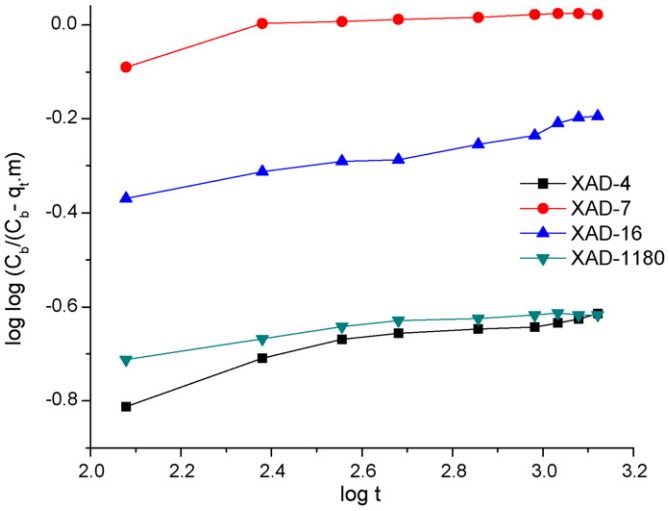

Fig. 7. Bangham plot for adsorption of Ginsenoside onto the sorbents.

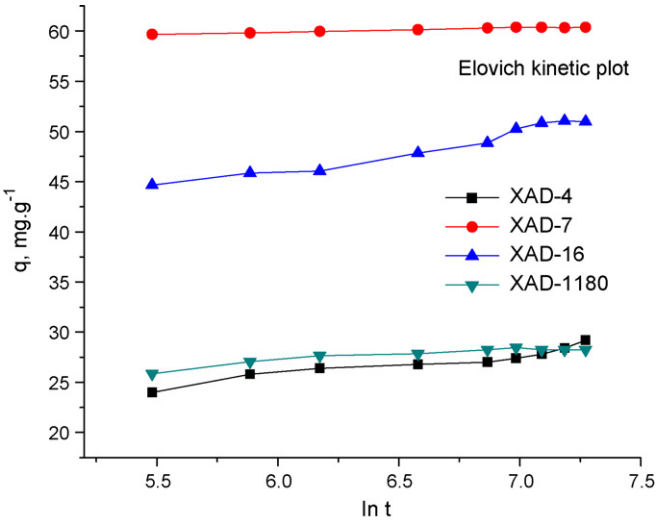

Fig. 8. Elovich model equation plot for adsorption of Ginsenoside.

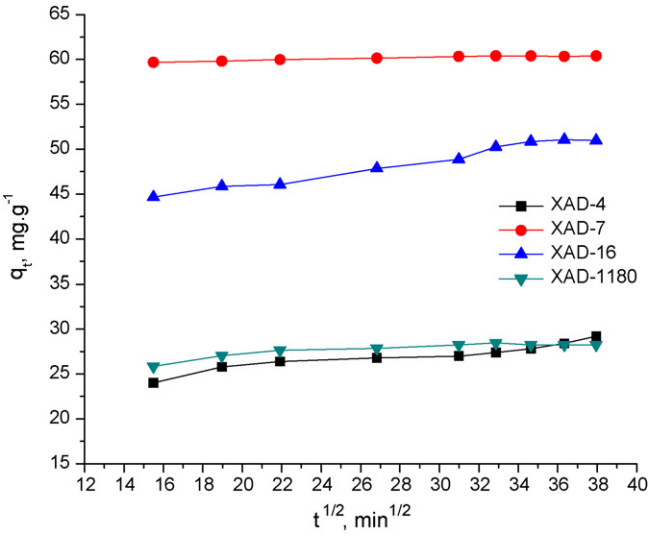

Fig. 9. Adsorption of Ginsenoside at 25 °C vs $t^{1/2}$ for different adsorbents.

time. Apparently, the data points in case of XAD-7 can be connected by a straight line, which indicates that the adsorption of Ginsenoside onto XAD-7 is controlled by a single rate controlling diffusion step. However, in the case of all other adsorbents, there are multi-linear plots depicting influence of two or more rate controlling steps in the sorption process. The first linear portion is for macropore or inter-particle diffusion and the second portion representing the micropore or intra-particle diffusion [30]. The intra-particle diffusion model parameters for sorption of Ginsenoside are evaluated and presented in Table 4. It is observed that the values of I and k_d are the highest and lowest in the series respectively in case of XAD-7. The Weber's model attributes significant influence by external

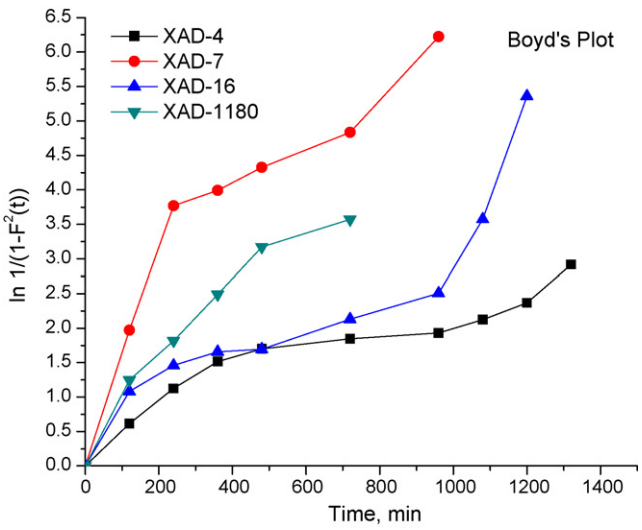

Fig. 10. Boyd's diffusivity plot for adsorption of Ginsenoside onto the sorbents.

mass transfer effect in the adsorption process on XAD-7 because of higher value of I [31,32].

Table 4 shows the values of effective diffusion coefficients (D_e) as calculated by Eq. (21) from the Boyd's Diffusivity Plot (Fig. 10). The values of D_e show that XAD-16 has the highest overall pore diffusion rate (7.77×10^{-13} m^2 s^{-1}). The Boyd's diffusion model also indicates that XAD-7 has less influence of pore diffusion in the adsorption process in comparison to XAD-16 resins. This is in support of the Weber's model for intra-particle diffusion, wherein the surface diffusion for Ginsenoside adsorption is observed to be significant in case of XAD-7 resins.

3.5. Effect of temperature and thermodynamic study

The effect of temperature on the adsorption process of Ginsenoside onto the polymeric Amberlite resins XAD-7 and XAD-16 was obtained by batch equilibrium experiments. It is observed that temperature has a distinct effect on the adsorption capacity of the adsorbents. Fig. 11 shows the plot of adsorption isotherm for Ginsenoside adsorption onto XAD-7 and XAD-16 resins at four different temperatures ranging from 293 to 308 K. It is observed that at lower adsorbate concentrations, the solute uptake increases sharply and thereafter the increase is gradual at higher concentrations. At 293 K, the adsorption capacity of both the resins is lower as depicted by the isotherm plots in Fig. 11. Experimental results also show that 298 K is the ideal temperature for both the resins in the adsorption process. Beyond 298 K, it is observed that with increase in temperature the adsorptivity decreases. This may be attributed for the exothermic nature of the sorption process and greater mobility of the molecules at elevated temperature and also possible desorption of some previously adsorbed molecules at higher temperature. In this regard it is noteworthy that the endothermic pore diffusion has less influence in the sorption process on both the adsorbents at the studied range of adsorbate concentration and temperature because

Table 4
Intra-particle diffusion model parameters and effective pore diffusivities for Ginsenoside adsorption onto various resins.

Adsorbents	Intra-particle diffusion model parameters			Effective pore diffusivities		
	k_d (mg g^{-1} min$^{-1/2}$)	I (mg g^{-1})	R^2	D_e (m^2 s^{-1})	R^2	R_a (m)
XAD-4	0.179	21.9	0.91	2.48×10^{-13}	0.88	2.95×10^{-4}
XAD-7	0.033	59.2	0.94	5.51×10^{-13}	0.83	2.73×10^{-4}
XAD-16	0.306	39.8	0.98	7.77×10^{-13}	0.85	3.75×10^{-4}
XAD-1180	0.092	25.1	0.79	2.49×10^{-13}	0.88	2.95×10^{-4}

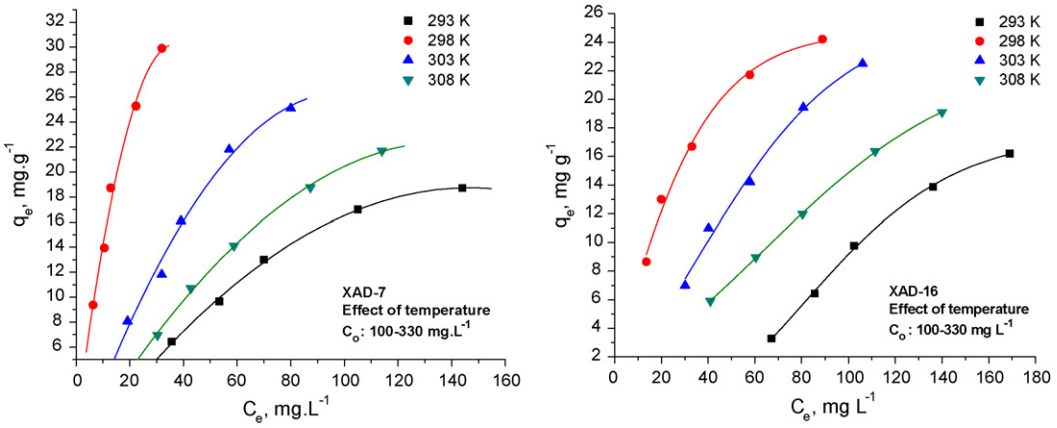

Fig. 11. Effect of temperature on adsorption of Ginsenoside on XAD-7 &16.

otherwise there would have been an increase in the adsorption capacity with temperature.

The isotherm parameters for three different isotherm models viz. Langmuir, Freundlich and Temkin models at different temperatures for Ginsenoside adsorption onto XAD-7 and XAD-16 are presented in Table 5 along with the values of the correlation coefficient. From the correlation coefficients ($R^2 > 0.9$) it appears that Temkin and Freundlich model best fits the experimental adsorption data for XAD-7 and XAD-16 resins and 298 K is the most preferred temperature for adsorption.

The values of entropy change (ΔS°) and enthalpy change (ΔH°) were obtained from intercept and slope of the plot of $\ln K_o$ versus $1/T$ (Fig. 12). The estimated values of the thermodynamic parameters for the three operating temperatures are presented in Table 6. The negative values of ΔG° confirm feasibility of Ginsenoside adsorption onto XAD-7 and XAD-16 surfaces and the negative values of ΔS° indicates non-spontaneity of the adsorption process. Negative value of ΔH° again indicates that the adsorption is exothermic in nature. It has also been observed that with rise in temperature the K_0 value decreases for adsorption onto both the resins.

The change in free energy for physical adsorption is normally in the range of −20 to 0 kJ mol^{-1} and is smaller than the chemisorption process which is in the range of −80 to −400 kJ/mol

Table 5
Isotherm parameters for Ginsenoside adsorption onto XAD-7 & 16 at different temperature.

Temp (K)	XAD-7			XAD-16		
	K_F (L mg^{-1})	$1/n$	R^2	K_F (L mg^{-1})	$1/n$	R^2
Freundlich isotherm parameters						
293	1.30×10^{-2}	0.127	0.97	0.05	1.16	0.95
298	2.62	0.721	0.97	2.14	0.60	0.97
303	0.70	0.832	0.98	0.41	0.90	0.98
308	0.42	0.845	0.98	0.23	0.93	0.99

Temp (K)	XAD-7			XAD-16		
	K_L (L mg^{-1})	q_m (mg g^{-1})	R^2	K_L (L mg^{-1})	q_m (mg g^{-1})	R^2
Langmuir isotherm parameters						
293	4.61×10^{-3}	49.2	0.83	5.74×10^{-3}	47	0.80
298	2.79×10^{-2}	64.7	0.94	2.75×10^{-2}	35	0.99
303	5.46×10^{-3}	85.8	0.73	4.75×10^{-3}	68	0.93
308	3.48×10^{-3}	79.0	0.76	1.18×10^{-3}	137	0.76

Temp (K)	XAD-7				XAD-16			
	B_1 (kJ^2 mol^{-2})	b (mol kJ^{-1})	K_T (L mg^{-1})	R^2	B_1 (kJ^2 mol^{-2})	b (mol kJ^{-1})	K_T (L mg^{-1})	R^2
Temkin isotherm parameters								
293	9.2	0.27	0.057	0.99	14.4	0.17	0.019	0.99
298	13.0	0.19	0.312	0.99	8.3	0.30	0.226	0.99
303	12.6	0.20	0.092	0.98	12.3	0.20	0.059	0.99
308	11.3	0.22	0.060	0.99	10.9	0.23	0.039	0.99

Table 6
Thermodynamic parameters for Ginsenoside adsorption onto XAD-7 & 16 resins.

Temp (K)	K_o		ΔH° (kJ mol^{-1})		ΔG° (kJ mol^{-1})		ΔS° (kJ mol^{-1} K^{-1})		R^2	
	XAD-7	XAD-16	XAD-7	XAD-16	XAD-7	XAD-16	XAD-7	XAD-16	XAD-7	XAD-16
298	13.5	4.88	−137	−92.7	−6.44	−3.93	−0.439	−0.298	0.95	0.99
303	3.8	2.41			−3.31	−2.18				
308	2.3	1.45			−2.01	−0.92				

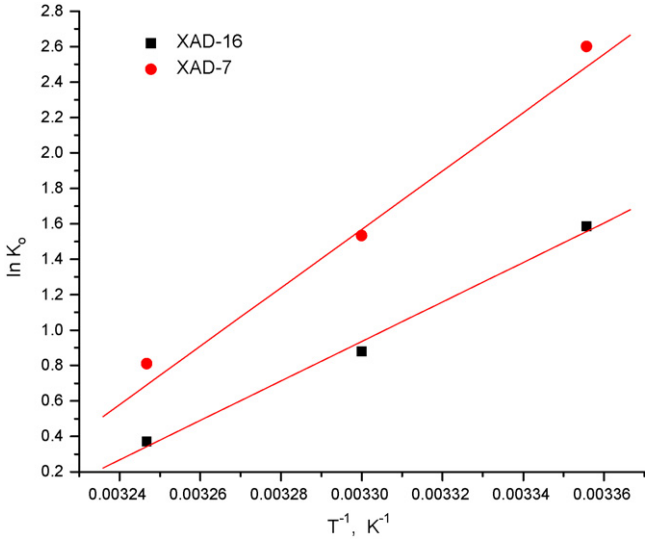

Fig. 12. Vant Hoff's thermodynamic plot for adsorption of Ginsenoside.

[33]. The changes in free energy of adsorption for the resins were estimated to be less than 0 kJ/mol, indicating occurrence of physio-sorption process [34]. The lower values of the free energy also indicate the feasibility of the adsorption process [35].

4. Conclusion

The present study shows that Amberlite non-ionic polymeric resins can be used as effective adsorbents for separation of Ginsenosides from aqueous solution. The removal effectiveness is in the order of XAD-7 > XAD-16 > XAD-1180 > XAD-4 and the equilibrium sorption was achieved in about 6 h. The adsorption efficiency and uptake rates of Ginsenoside onto various resins were compared and the highest adsorption efficiency and rate were observed with XAD-7. The optimum adsorbent doses for all the adsorbents were found to be 10–15 g L^{-1} with uniform adsorption at a concentration of 0.33 g L^{-1} Ginsenoside. Five different isotherm models provided by Langmuir, Freundlich, Redlich Peterson, Dubinin Radushkevich and Temkin were used to fit the experimental equilibrium data for sorption of aqueous Ginsenoside onto four different polymeric adsorbents, XAD-4,7,16 and 1180. The observed profiles of solid phase concentration of Ginsenoside at equilibrium, onto the resins against the liquid phase concentration C_e, indicate a good fit for the Langmuir, Freundlich, Redlich Peterson and the Temkin models to the experimental data verifying that the adsorption processes are favourable. The mean free energy of adsorption was estimated using the Polanyi Potentiali and the D-R isotherm constants and were in the range of 0.04–0.26 kJ mol^{-1} signifying occurrence of physical adsorption. The thermodynamic study conducted on the most effective resins XAD-7 and 16, showed that adsorption is characterized by uniform distribution of binding energy. The uptake of Ginsenoside increases with temperature, the optimum temperature of adsorption being 298 K. The estimated values of ΔG° confirm feasibility of Ginsenoside adsorption onto XAD-7 and 16 and the negative values of ΔS° indicates non-spontaneity of the adsorption process. Negative value of ΔH° designates the adsorption process to be exothermic. The adsorption study also reveals that the diffusion of the adsorbate into the pores is not the only rate controlling step and both film and pore-diffusion play significant role to different extent and stages of contact in the sorption process. XAD-7 has significant influence of external mass transfer effect in the adsorption process of Ginsenoside.

Appendix A. Nomenclature

q	amount of solute per unit mass of adsorbent (mg g^{-1})
q_e	equilibrium solute phase concentration in adsorbate (mg g^{-1})
q_t	concentration of adsorbate in solid phase at time t (mg g^{-1})
q_m	Langmuir equation constant (mg g^{-1})
C_0	initial liquid phase concentration of solute (mg L^{-1})
C_e	equilibrium solute concentration in liquid (mg L^{-1})
C_{ad}	reduction of adsorbate concentration of solution at equilibrium (mg L^{-1})
V	volume of the solution (L)
m	mass of the adsorbent (g)
K_L	constant of Langmuir isotherm (mL mg^{-1})
R_L	Langmuir dimensionless factor
K_F	constant of Freundlich isotherm (ml^n mg$^{(1-n)}$ g^{-1})
n	Freundlich isotherm parameter (dimensionless)
K_R	Redlich–Peterson isotherm constants (L g^{-1})
a_R	Redlich–Peterson parameter (L $mg^{-1})^{-1/\beta}$
β	Redlich–Peterson dimensionless parameter
Q_D	Dubinin–Radushkevich isotherm constant (mg g^{-1})
ε	Polanyi Potentiali (kJ mol^{-1})
B_D	Dubinin–Radushkevich equation parameter (mol^2. kJ^{-2})
E	mean free energy of sorption (kJ mol^{-1})
K_T	equilibrium binding constant (L mg^{-1})
b	Temkin isotherm constant (mol kJ^{-1})
k_f	rate constant of pseudo-first-order adsorption reaction (min^{-1})
t	time (h)
T	temperature (K)
k_s	rate constant for pseudo-second-order adsorption reaction (g mg^{-1} min^{-1})
C_b	initial adsorbate in the liquid phase (mg)
k_0	Bangham's equation parameter (L g^{-1})
σ	Bangham's equation dimensionless parameter
k_d	intra-particle diffusion rate constant (mg g^{-1} $min^{-½}$)
D_e	Boyd's rate constant (m^2 s^{-1})
R_a	radius of the spherical adsorbent particle (m)
α	initial adsorption rate
ω	adsorption rate
ΔH°	enthalpy of adsorption (kJ mol^{-1})
ΔG°	Gibb's free energy of adsorption (kJ mol^{-1})
ΔS°	entropy change (J mol^{-1} K^{-1})
R	universal gas constant (8.314 J mol^{-1} K^{-1})
K_0	thermodynamic equilibrium constant at temperature T

References

[1] K.W. Yu, H.N. Murthy, E.J. Hahn, K.Y. Paek, Ginsenoside production by hairy root cultures of Panax ginseng: influence of temperature and light quality, Biochem. Eng. J. 23 (2005) 53–56.
[2] W. Tang, G. Eisenbrand, Panax Ginseng, C.A. Mayer, Chinese Drugs of Plant Origin, Springer, Berlin, 1992, pp. 710–737.
[3] C. Zhang, H. Yu, Y. Bao, L. An, F. Jin, Purification and characterization of Ginsenoside-β-Glucosidase, Chem. Pharm. Bull. 49 (2001) 795–798.
[4] Q. Fang, H.W. Yeung, H.W. Leung, C.W. Huie, Micelle-mediated extraction and pre-concentration of ginsenosides from Chinese herbal medicine, J. Chromatogr. A 904 (2000) 47–55.
[5] P. Barkakati, S. Borthakur, M. Borthakur, M. Bordoloi, N.C. Baruah, P. Phukan, H.P. Sarmah, P.G. Rao, A. Mathur, A.K. Mathur, A.K. Kukreja, Efficient recovery of composite ginsenoside from bioreactor harvest of cultured Panax quinquefolium cells, Ind. Pat. Appl. (2009), No. 031NF.
[6] Q. Lang, C.M. Wai, An extraction method for determination of ginkgolides and bilobalide in ginkgo leaf extracts, Anal. Chem. 71 (1999) 2929–2933.
[7] M.A. Abdullah, L. Chiang, M. Nadeem, Comparative evaluation of adsorption kinetics and isotherms of a natural product removal by Amberlite polymeric adsorbents, Chem. Eng. J 146 (2009) 370–376.

[8] M.H.L. Ribeiro, D. Silveira, S. Ferreira-Dias, Selective adsorption of limonin and naringin from orange juice to natural and synthetic adsorbents, Eur. Food Res. Technol. 215 (2002) 462–471.
[9] M.D. Saikia, Revisiting adsorption of biomolecules on polymeric resins, Colloids Surfaces A: Phys. Chem. Eng Aspects 315 (2008) 196–220.
[10] H. Wang, Z. Fei, J. Chen, Q. Zhang, Y. Xu, Adsorption thermodynamics and kinetic investigation of aromatic amphoteric compounds onto different polymeric adsorbents, J. Environ. Sci. 19 (2007) 1298–1304.
[11] N. Fuzzati, Analysis methods of ginsenosides, J. Chromatogr. B 812 (2004) 119–133.
[12] M.P. Gomez-Serranillos, O.M. Palomino, E. Carretero, A. Villar, M.A. Cases, A new HPLC method for the analysis of ginsenosides in Panax ginseng, Fitoterapia (Milano) 68 (1997) 533–536.
[13] I. Langmuir, The constitution and fundamental properties of solids and liquids, J. Am. Chem. Soc. 38 (1916) 2221.
[14] H. Freundlich, Über die adsorption in iösungen, J. Phys. Chem. 57 (1907) 385–470.
[15] O. Redlich, D.L. Peterson, A useful adsorption isotherm, J. Phys. Chem. 63 (1959) 1024–1026.
[16] M.M. Dubinin, L.V. Radushkevich, Equation of the characteristic curve of activated charcoal, Chemisches Zentralb latt. 1 (1947) 875–889.
[17] M.J. Temkin, V. Pyzhev, Kinetics of ammonia synthesis on promoted iron catalysis, Acta Physicochim, USSR 12 (1940) 217–222.
[18] S. Lagergren, Zur theorie der sogenannten adsorption gelöster stoffe, Kungliga Svenska Vetenskapsakademiens, Handlingar 24 (1898) 1–39.
[19] Y.S. Ho, G. McKay, Kinetic model for lead (II) sorption onto peat, Adsorpt. Sci. Technol. 16 (1998) 243–255.
[20] C. Aharoni, S. Sideman, E. Hoffer, Adsorption of phosphate ions by colloid ion-coated alumina, J. Chem. Technol. Biotechnol. 29 (1979) 404–412.
[21] W.J. Weber Jr., J.C. Morris, Kinetics of adsorption on carbon from solutions, J. Sanitary Eng. Div. ASCE 89 (1963) 31–60.
[22] G.E. Boyd, A.W. Adamson, L.S. Mayers Jr., The exchange adsorption of ions from aqueous solutions on organic zeolites: II Kinetics, J. Am. Chem. Soc. 69 (1947) 2836–2848.
[23] S.Z. Roginsky, Ya. Zeldovich, Acta Phys. Chem. USSR 1 (1934) 554.
[24] S.H. Chien, W.R. Clayton, Application of Elovich equation to the kinetics of phosphate release and sorption on solids, Am. J. Soil Sci. Soc. 44 (1980) 265–268.
[25] T.W. Weber, R.K. Chakraborty, Pore and solid diffusion models for fixed bed adsorbents, J. Am. Inst. Chem. Eng. 20 (1974) 228–238.
[26] S.D. Faust, O.M. Aly, Adsorption processes for water treatment, Butterworths, 1987.
[27] M. Mahramanlioglu, I. Kizilcikli, I.O. Bicer, Adsorption of fluoride from aqueous solution by acid treated spent bleaching earth, J. Fluorine Chem. 115 (2002) 41–47.
[28] Y. Kim, C. Kim, I. Choi, S. Rengraj, J. Yi, Arsenic removal using mesoporous alumina prepared via a templating method, Environ. Sci. Technol. 38 (2004) 924–931.
[29] E. Tutem, R. Apak, C.F. Unal, Adsorptive removal of chlorophenols from water by bituminous coal, Water Res. 32 (1998) 2315–2324.
[30] S.J. Allen, G. Mckay, K.Y.H. Khader, Intraparticle diffusion of a basic dye during adsorption onto sphagnum peat, Environ. Pollut. 56 (1989) 39–50.
[31] G. McKay, M.S. Otterburn, A.G. Sweeney, The removal of colour from effluent using various adsorbents III Silica: rate processes, Water Res. 14 (1980) 15–20.
[32] J. Crank, The Mathematics of Diffusion, Second ed, Oxford: Clarendon Press, London, 1975.
[33] M.J. Jaycock, G.D. Parfitt, Chemistry of Interface, Ellis Howard, Orichester, 1981, pp. 12–13.
[34] M.G. Roig, Sorption processes, in: J.F. Kennedy, J.M.S. Cabral (Eds.), Recovery Processes for Biological Materials, Willey, Chichester, 1993, pp. 369–414.
[35] M.S. Bilgili, Adsorption of 4-chlorophenol from aqueous solutions by xad-4 resin: isotherm, kinetic and thermodynamic analysis, J. Hazard. Mater. B137 (2006) 157–164.